IJRCS

International Journal of Robotics and Control Systems
Vol. 5, No. 2, 2025, pp. 1120-1138
ISSN 2775-2658
http://pubs2.ascee.org/index.php/ijrcs

ASCEE

Enhancing MG996R Servo Motor Performance Using PSO-Tuned PID and Feedforward Control

Phichitphon Chitikunnan [a,1], Yutthana Pititheeraphab [a,2,*], Thanate Angsuwatanakul [a,3], Jaroonrut Prinyakupt [a,4], Tasawan Puttasakul [a,5], Rawiphon Chotikunnan [a,6], Nuntachai Thongpance [a,7]

[a] College of Biomedical Engineering, Rangsit University, Pathum Thani 12000, Thailand
[1] phichitphon.c@rsu.ac.th; [2] yutthana.p@rsu.ac.th; [3] thanate.a@rsu.ac.th; [4] jaroonrut.p@rsu.ac.th; [5] tasawan.p@rsu.ac.th; [6] rawiphon.c@rsu.ac.th; [7] nuntachai.t@rsu.ac.th
* Corresponding Author

ARTICLE INFO

Article history
Received March 20, 2025
Revised April 21, 2025
Accepted April 29, 2025

Keywords
MG996R Servo Motor;
PSO-PID Optimization;
Feedforward Control;
Real-Time Position Tracking

ABSTRACT

The aim of this research is to improve the precision of factory-locked MG996R servo motors, which are frequently employed in biomedical and robotic applications. These motors are characterized by the absence of inherent feedback channels and adjustable internal settings. The proposed technique proposes a non-invasive control strategy that utilizes externally obtained feedback to enable closed-loop control without requiring any modifications to the interior circuitry. The scientific contribution consists of the development of an outer-loop PID control framework that has been optimized using Particle Swarm Optimization (PSO) and enhanced with feedforward compensation. By utilizing the inherent potentiometer, this method ensures the preservation of hardware integrity and enables real-time angle feedback. A model fit of 96.94% was achieved by establishing a second-order discrete-time model using MATLAB's System Identification Toolbox. Particle Swarm Optimization (PSO) was employed to optimize PID improvements offline by minimizing the Integral of Squared Error (ISE). In both experimental and simulated environments, the controller's effectiveness was assessed using 2 rad/s sine wave inputs and a 10° step. The PSO-PID with feedforward controller achieved optimal results, achieving an RMSE of 0.5313° and an MAE of 0.1630° in simulations, as well as an MAE of 0.8497° in hardware step response. The requirement for gain scaling in embedded systems was underscored by the instability of the standalone PSO-PID controller. This method offers a pragmatic, scalable solution for applications such as assistive robotics, prosthetic joints, and surgical instruments. In order to achieve sub-degree precision in safety-critical environments, future endeavors will entail the implementation of adaptive gain tuning and enhanced resolution sensing.

1. Introduction

Servo motors, especially economical variants like the MG996R, are extensively employed owing to their small architecture, cost-effectiveness, and built-in control electronics [1], [2]. These motors often have an inbuilt proportional (P) controller, rendering them appropriate for fundamental position control duties but limited when used with externally implemented PID enhancements [3]. Advanced

implementations like GWO-PID for hybrid stepping motors and intelligent wheelchair control systems have significantly broadened the functional scope of servo motors beyond fundamental tasks [4], [5].

Nonetheless, their rigid internal control architecture presents considerable obstacles for applications requiring high accuracy, stability, and flexibility, including robotic arms, exoskeletons, humanoid robots, and therapeutic robotic devices [6]-[9]. Many industrial and biomedical applications frequently lack access to or the capacity to adjust internal servo settings, thereby constraining the potential to improve control precision and adaptability in dynamic environments [10], [11]. Numerous studies have proposed external PID controllers to address these limitations; however, they often depend on manual gain tuning, which may be inefficient and result in diminished performance in dynamically evolving situations [12]-[14].

In order to overcome the limitations of human calibration in external PID control, recent research has increasingly implemented optimization-based methodologies to automate gain selection and improve system performance. Methods such as fuzzy-PID optimization [15]-[17], conventional and hybrid PID implementations [18]-[20], and sophisticated techniques like Particle Swarm Optimization (PSO) [21]-[23] have demonstrated substantial improvements in tracking precision, real-time flexibility, and convergence rate. Specifically, PSO has become a preferred tuning algorithm owing to its simplicity and shown effectiveness in several control contexts, including motor regulation and process dynamics [24]-[26].

Moreover, hybrid control paradigms that integrate fuzzy logic with PID frameworks (fuzzy-PID) [27]-[29], alongside intelligent models employing neural networks [30], [31], and fractional-order control approaches [32]-[35], have demonstrated enhanced adaptation to nonlinear and unpredictable system dynamics. These approaches have been effectively used across several robotic platforms, including manipulators [36], assistive and rehabilitative devices [37], self-balancing mobile robots [38], embedded systems, and electric vehicle control frameworks [39], [40]. Nonetheless, the majority of these solutions presuppose the existence of internal control access or adaptable feedback topologies, rendering them less suitable for factory-locked servo motors like the MG996R.

This work addresses this gap by presenting a viable external control technique that preserves internal hardware integrity while enhancing accuracy using a PSO-tuned PID controller with feedforward integration. Although there has been significant advancement in the field of servo motor control, most current methods are dependent on advanced embedded architectures or internally reconfigurable components. These requirements are unsuitable for factory-locked servo motors such as the MG996R, which often exhibit nonlinearities, mechanical dead zones, and inaccessible internal feedback mechanisms. These constraints considerably hinder control accuracy and responsiveness, especially in biomedical robotic applications requiring high precision.

In previous research, the limitations imposed by the absence of internal control access have not been sufficiently addressed. These studies have primarily concentrated on mechanical integration and general control frameworks that employ MG996R actuators in bio-inspired snake robots [41] and low-cost educational robotic arms [42]. This study suggests an external PSO-tuned PID control architecture with feedforward compensation as a solution to these constraints. By externally acquiring feedback from the internal potentiometer, this method preserves factory integrity and extends servo functionality, thereby enabling high-precision angular control without modifying the original circuitry.

Practical issues, such as the computational burden of PSO optimization and the challenges of real-time gain adaptation, persist in spite of these advantages. Algorithmic simplification and efficient implementation are necessary to resolve these issues. This research makes a significant contribution by providing two key components: (1) a non-invasive, externally mountable control strategy for constrained servo systems, and (2) experimental validation through comprehensive simulations and hardware testing. While other research has explored external feedback integration [43] or fuzzy-PID tuning for enhanced performance [44], only a few have directly tackled the specific mechanical and

electrical limitations of fixed-architecture servo motors. Although this approach is not limited to MG996R, it enriches the broader domain of externally enhanced, factory-intact servo motor control systems [45], [46].

This research augments and expands upon previous research on intelligent control in drone systems, microgrids, and assistive robotics, leveraging these insights to address factory-locked servo constraints. It illustrates the efficacy of PSO in the regulation of thermal and motor systems by employing the Integral of Squared Error (ISE) criterion to optimize PID gain [50]-[52]. The incorporation of feedforward compensation enhances system responsiveness and minimizes steady-state error, as demonstrated in previous research on fuzzy-PID-controlled servo systems [53]-[55].

In order to assess the proposed method, a series of physical experiments and simulations were conducted in embedded platforms and multi-DOF systems, utilizing both step and sinusoidal references [56]-[58]. The proposed PSO-PID with feedforward consistently achieved lower steady-state errors, speedier rise times, and smoother trajectory tracking than the factory-default proportional control, manually tuned PD, and standalone PSO-PID, as demonstrated by performance comparisons [59]-[62]. Nevertheless, the necessity of gain scaling in embedded multi-actuator environments such as exoskeletons and autonomous robotic systems was underscored by the instability of standalone PSO-PID control under practical conditions, which was attributed to excessive integral action [63]-[67].

The contributions of this study are threefold. Initially, it introduces a non-invasive control method for factory-locked servo motors, employing PSO-tuned PID with feedforward compensation. This method requires no alterations to the internal circuitry, hence enhancing the motor's control capabilities while preserving its original integrity. Secondly, the suggested methodology is validated by simulations and hardware experiments, with performance assessments compared to conventional P, manually calibrated PD, and autonomous PSO-PID controllers utilizing both step and sinusoidal reference signals. The study highlights practical difficulties, particularly instability caused by excessive integral action in PSO-PID controllers that do not incorporate feedforward correction. These results underscore the necessity of integrating predictive mechanisms to enhance the overall stability of the system. The system exhibits notably enhanced robustness, faster response time, and higher tracking precision by utilizing a PSO-tuned PID controller with feedforward and internally accessed potentiometer feedback. In biomedical robotic applications, such as rehabilitation devices, assistive exoskeletons, prosthetic limbs, and surgical instruments, sub-degree control accuracy directly impacts safety and therapeutic outcomes. Consequently, such enhancements are particularly critical. This research provides new opportunities for the development of low-cost, real-time, multi-axis control solutions in constrained embedded environments.

2. Method

The objective of this investigation is to assess the effectiveness of external control methods on a pre-configured servo motor (MG996R) that typically utilizes internal proportional (P) control. The procedure comprises four primary steps: (1) modifying the system and establishing feedback; (2) determining the transfer function; (3) devising a control scheme; and (4) fine-tuning the PID controller using Particle Swarm Optimization (PSO).

The implementation of a PSO-tuned PID controller with feedforward integration is the primary methodology employed in this research to improve the control performance of factory-locked MG996R servo motors, as illustrated in Fig. 1. The process commences with the meticulous opening of the servo casing and the routing of an external wire from the internal potentiometer, known as servo motor preparation. This avoids the modification of the internal control circuitry, thereby preserving the motor's original structure by providing access to real-time angular feedback.

The subsequent phase, data acquisition, entails the transmission of PWM command signals to the servo and the subsequent recording of the corresponding feedback voltages from the potentiometer. These time-domain input-output data are subsequently employed in the system identification phase,

during which MATLAB's System Identification Toolbox is employed to model a second-order discrete-time transfer function. The subsequent controller design is based on the resulting model, which obtains a fit accuracy of 96.94%.

PSO-based PID optimization is implemented offline in MATLAB subsequent to identification. Optimal PID gains are determined by minimizing the Integral of Squared Error (ISE) through Particle Swarm Optimization. In order to guarantee convergence, parameters such as the search space for K_p, K_i, and K_d, as well as the number of iterations and swarm size, are established.

Two controller architectures are developed during the controller design phase: a standard feedback-only PID controller and a feedforward-augmented version. These architectures are subsequently subjected to the optimized advances. Modeling The tracking accuracy, transient response, and steady-state behavior are assessed through testing conducted under two reference inputs: a 10° step and a 2 rad/s sine wave. RMSE, MAE, overshoot, and rise time are all performance metrics.

Hardware implementation is implemented subsequent to simulation validation. In order to accommodate the Arduino Uno's memory and computational limitations, the PID gains are appropriately reduced. The real-world responses are recorded after the controllers are verified with the physical MG996R motor.

Finally, the Results Comparison & Analysis phase evaluates the results of both the simulation and the experiment. This section addresses discrepancies that are the result of hardware nonlinearities, including gear backlash, dead-zone effects, and sensor noise.

Lastly, the Conclusion and Future Work stage provides a summary of the primary findings and suggests potential future research directions. These include the extension of the method to multi-axis systems, the implementation of adaptive gain tuning, and the resolution of hardware-specific nonlinearities to further improve the precision and robustness of the system in biomedical and robotic applications.

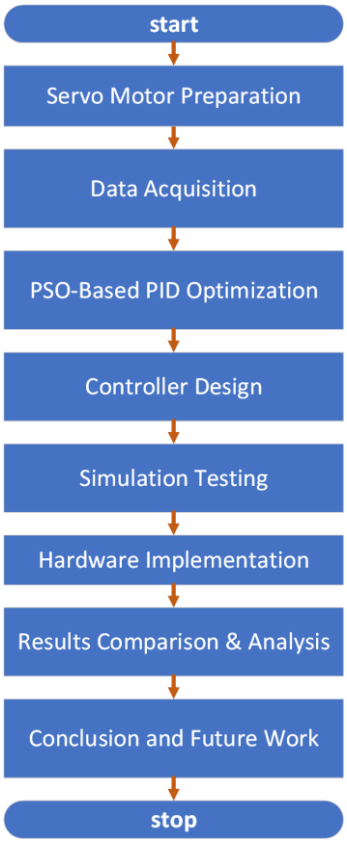

Fig. 1. Research flowchart: PSO-PID with feedforward control for MG996R servo

2.1. Servo Motor

The servo motor adopted in this study, seen in Fig. 2, is the MG996R, a commonly used standard servo recognized for its small dimensions, cost-effectiveness, and straightforward integration. Typical applications encompass robotic arms, surgical equipment akin to the Da Vinci system, small robotic appendages, and robotic prosthetic hands as seen in Fig. 2.

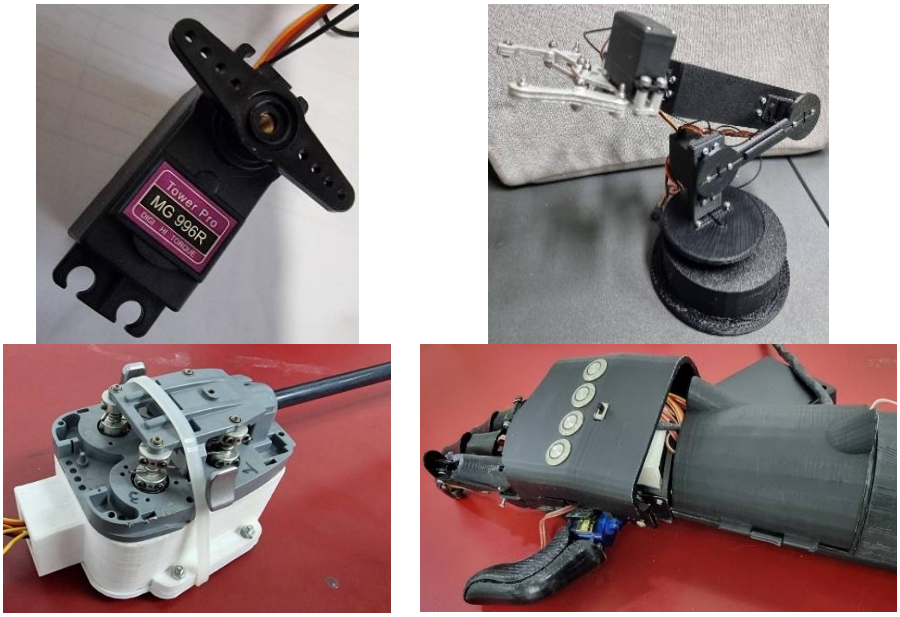

Fig. 2. MG996R servo motor and example applications of servo motors

This study modified the servo by routing a signal wire directly from the internal potentiometer (VR), which provides the position reference to the internal controller, to facilitate external feedback acquisition. This approach does not disrupt the current internal control circuit and enables real-time angular feedback for external processing. The analog-to-digital converter (ADC) of an Arduino Uno was directly connected to the potentiometer's output without the use of a buffering circuit. The angular displacement of the servo shaft was linearly represented by the observed voltage range, which ranged from 0 to 3.3 volts, as illustrated in Fig. 3.

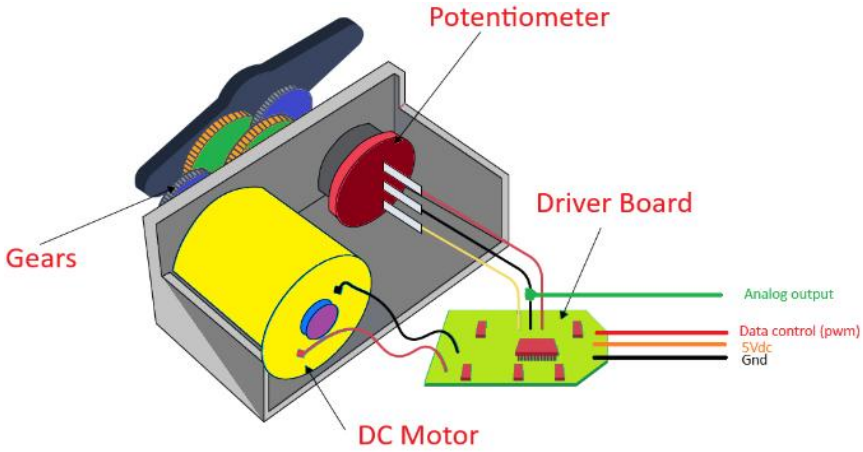

Fig. 3. External feedback acquisition from the internal potentiometer of the MG996R

2.2. Transfer Function of Servo Motor Systems

This study used a system identification approach in MATLAB to determine the transfer function of the MG996R servo motor system. The methodology employed time-domain input and output data with a sampling interval of 0.01 seconds (10 ms). The input signal was a Pulse Width Modulation

(PWM) command signal, as shown in Fig. 4, while the output was an analog voltage signal acquired via external feedback acquisition from the internal potentiometer, representing the angular position of the motor shaft.

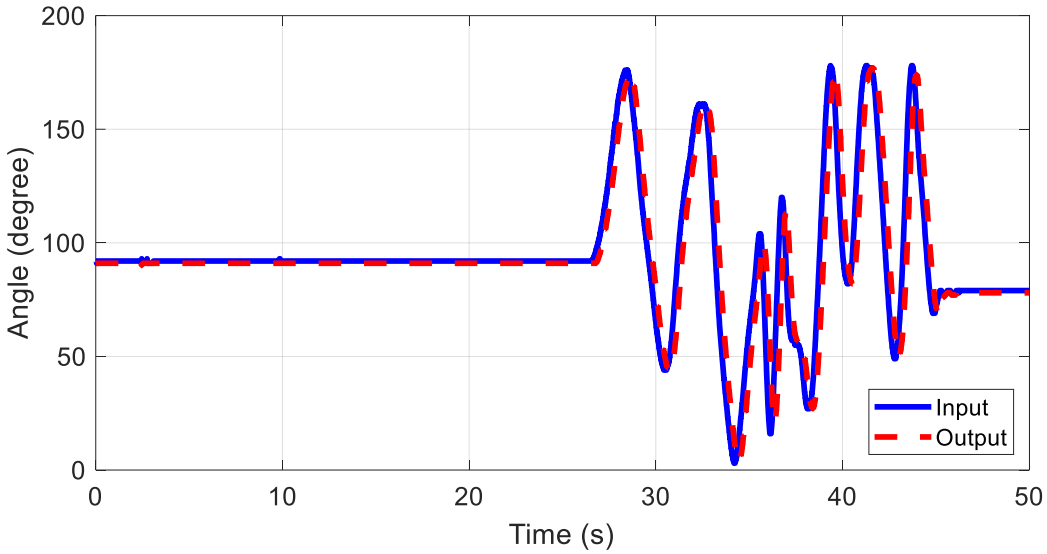

Fig. 4. Servo motor input (PWM) and output (analog position feedback)

The servo motor's discrete-time transfer function was estimated using the "tfest" function in MATLAB. Commercial servo motors, such as the MG996R, possess fixed internal proportional (P) controllers, which inhibit modifications to internal control parameters. This study addressed that constraint by non-invasively obtaining internal feedback, facilitating accurate external characterization of the closed-loop behavior. The resultant second-order transfer function model is presented as (1).

$$G(z) = \frac{0.01411z}{z^2 - 1.829z + 0.8429} \quad (1)$$

The identification and capture of this model with a 10 ms sampling interval resulted in a mean squared error (MSE) of 0.5411. Two poles and one zero comprise the paradigm. The model fit was 96.94% accurate, making it suitable for control design and simulation. Despite the model's presumption of linear behavior, nonlinearities may be introduced by real-world characteristics of the MG996R, such as gear backlash and saturation. By employing authentic input-output data, these effects were alleviated during offline PSO optimization. Dead-zone or hysteresis modeling may be explicitly incorporated in future research. The optimization process converged rapidly, requiring three iterations and seven function evaluations. This suggests that the identified system is deterministic and well-behaved. The close correlation between the actual and estimated behaviors is demonstrated in Fig. 5, which displays both the measured output and the predicted model response. The structural block diagram of the servo motor control system is also provided in the bottom panel, which illustrates the relationship between the external observation loop, potentiometer-based feedback, internal servo processing, and input PWM signals.

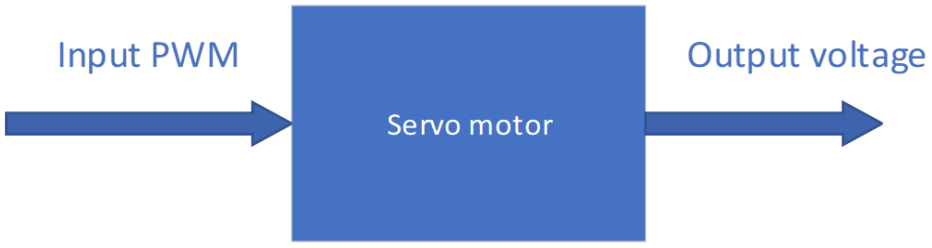

Fig. 5. Illustrates the structural block diagram of servo motor

2.3. Feedback Control Design

In order to optimize the functionality of factory-configured MG996R servo motors, this investigation necessitated the development of a closed-loop control system. Modifications to the internal gain are frequently prohibited by the proportional (P) controller that is integrated into these motors. These constraints necessitate precise external control for applications that necessitate sub-degree accuracy, a requirement that is common in biomedical and robotic applications, including medical assistive devices, robotic arms, and prosthetic appendages. In order to enhance the stability and accuracy of the control system, a discrete-time PID controller was implemented.

The PID controller has three control actions: proportional (P), integral (I), and derivative (D). These are used together to figure out the control signal, which is based on the difference between the input reference and the output of the system. The control legislation is specified in (2).

$$u_j(k) = K_p e_j(k) + K_i \sum_{n=k-N}^{k} e_j(n) + K_d \left(e_j(k) - e_j(k-1)\right) \tag{2}$$

In this context, $u_j(k)$ denotes the control signal at time step k, whereas $e_j(k)$ indicates the deviation between the reference and the actual output. The proportional, integral, and derivative components are represented by the gain parameters K_p, K_i, and K_d, respectively. These components are designed to improve the system's responsiveness to dynamic variations, eradicate steady-state error, and reduce rise time. The feedback-only control system is configured as depicted in Fig. 6.

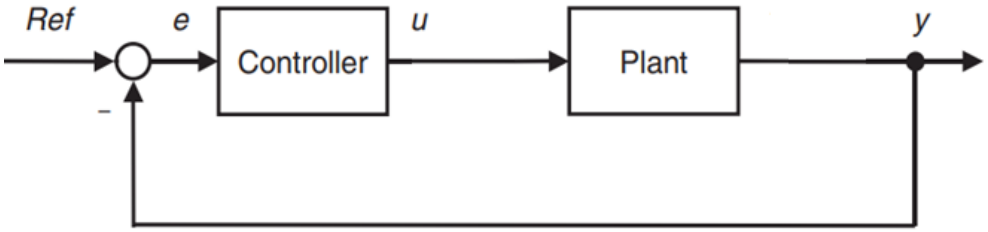

Fig. 6. Standard PID feedback control structure

In addition to the feedback-only control, this study looked at how to build a feedforward-enhanced PID controller to make the system more responsive. The feedforward architecture has a predictive control element to offset expected variations in the reference signal. In this design, the PID feedback is included in the reference input, resulting in the subsequent control law.

$$u_j(k) = \text{Ref}(k) + \left(K_p e_j(k) + K_i \sum_{n=k-N}^{k} e_j(n) + K_d \left(e_j(k) - e_j(k-1)\right) \right) \tag{3}$$

This feedforward technique enables the system to respond more swiftly to anticipated input variations, which is particularly beneficial in systems characterized by rapid dynamics or time-sensitive responses. Fig. 7 illustrates the block diagram of this advanced feedforward-PID control configuration.

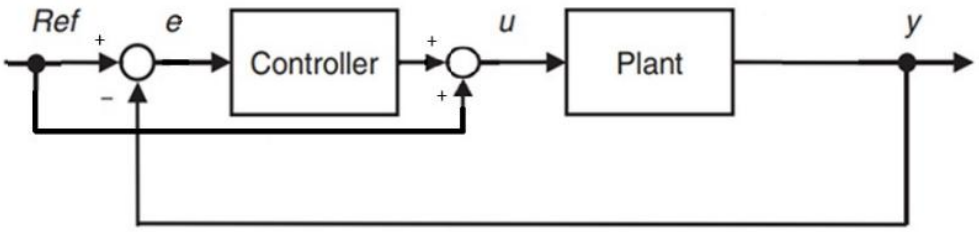

Fig. 7. Feedforward-augmented PID control structure

To determine optimal PID gain values (K_p, K_i, K_d), this study employed Particle Swarm Optimization (PSO). The objective function minimized was the Integral of Squared Error (ISE) between the reference and the output signal during simulation-based evaluation using the identified servo motor model.

2.4. PID Tuning via Particle Swarm Optimization (PSO)

The optimal gain parameters (K_p, K_i, K_d) for the discrete-time PID controller utilized in this study were determined using the global optimization method of Particle Swarm Optimization (PSO). The PSO algorithm is a metaheuristic that is inspired by the social behavior of avian flocking or fish schooling. It facilitates efficient global search without the necessity of gradient information. Two control architectures were evaluated: the first was a PID feedback-only architecture, and the second was a feedforward-enhanced PID architecture. The controller modulates the plant by exploiting the discrepancy between the reference and the output in the feedback-only scenario. The cost function was defined as the Integral of Squared Error (ISE) between the reference and feedback output, and the control input was calculated as (1).

In the feedforward-enhanced design, which incorporated a predictive control element, a pseudo-error was calculated by comparing the reference and the prior output. This was achieved by explicitly incorporating the feedforward control signal into the PID feedback controller, which allowed the system to anticipate and mitigate input disturbances. The identical PSO-based methodology was implemented in this configuration to mitigate ISE.

The empirically selected gain search ranges were as follows: $K_p \in [0, 5], K_i \in [0, 20], and\ K_d \in [0, 2]$. The PSO was configured with a swarm of 30 particles and 50 iterations in preliminary simulations, which were sufficient for global convergence. The system's response to a 10-degree step input was simulated to confirm the optimal gains that were attained. The system's efficacy was evaluated by implementing the following parameters: steady-state error, overshoot, settling time, and rise time.

This method simplifies controller calibration, even when applied to plant models that exhibit nonlinearities or time-variant behavior, which are common in servo-based embedded systems. The microcontroller was used to scale and deploy the optimized gains, as the computational complexity of PSO necessitated offline modification in MATLAB. Real-time implementation of PSO was not attempted due to processing and memory constraints of Arduino Uno. The pseudocode of the PSO algorithm that was implemented for PID optimization is depicted in Fig. 8. The optimal parameters for the feedback-only PID control were K_p = 5, K_i = 20, and K_d = 0.5981, as indicated by the simulation results. This produced a cumulative ISE of 227.8931. The ideal parameters for the feedforward-enhanced PID control were K_p = 5, K_i = 0, and K_d = 0.6352, yielding a final ISE of 203.3357. This study's results demonstrate that the integration of feedforward compensation improves dynamic performance and tracking accuracy, especially in transient response situations.

The findings highlight the efficacy of PSO for embedded PID tuning, especially in factory-locked servo systems whose internal control parameters cannot be altered after production.

3. Results and Discussion

To assess system performance, two types of input signals were utilized: a 10-degree step input and a sine wave input with an angular frequency of 2 rad/s (about 0.318 Hz in standard frequency). The assessment was performed using modeling and empirical analysis of the MG996R servo motor. There are four different control configurations shown in Fig. 9. The first is the factory-default control, which uses an internal proportional (P) control that has not been changed. The second is a PSO-optimized PID control (K_p = 5, K_i = 20, K_d = 0.5981), where the gain parameters were improved through particle swarm optimization. The third is a manually calibrated PD control (K_p = 5, K_i = 0, K_d = 0.5981), where only the proportional and derivative gains were changed. The fourth is a PSO-

optimized PID controller with a feedforward term (K_p= 5, K_i = 0, K_d = 0.6352), which was added to improve the accuracy of tracking the reference trajectory. The feedforward component mitigated phase lag and motor inertia effects, which enhanced tracking performance, especially under sinusoidal excitation. Under hardware implementation, the gain values derived by PSO were reduced by a factor of four to guarantee system stability under real-world settings. This scaling was necessary due to overshooting and instability caused by high integral gains in practical deployment, highlighting the limitations of directly porting simulation-optimized gains into resource-constrained embedded systems.

Initialize parameters:
- **Number of particles**: N
- **Number of dimensions**: $D = 3 \rightarrow [K_p, K_i, Kd]$
- **Maximum iterations**: *maxIter*
- **Inertia weight**: w
- **Cognitive coefficient**: c_1
- **Social coefficient**: c_2
- **Search space bounds**:
  - $K_p \in [K_{p-min}, K_{p-max}]$
  - $K_i \in [K_{i-min}, K_{i-max}]$
  - $Kd \in [Kd_{-min}, Kd_{-max}]$

Initialize particles:
For i = 1 to N:
- Randomly initialize **position** $\mathbf{x}_i = [K_{pi}, K_{ii}, Kd_i]$
- Randomly initialize **velocity** $\mathbf{v}_i$
- Evaluate **cost function** J_i = ISE(PID with $\mathbf{x}_i$)
- Set **personal best** $\mathbf{pbest}_i = \mathbf{x}_i$
- Set **personal best cost** $J\_\mathbf{pbest}_i = J_i$

Set global best:
- $\mathbf{gbest}$ = $\mathbf{pbest}_i$ with minimum $J\_\mathbf{pbest}_i$

Repeat for each iteration t = 1 to *maxIter*:
For each particle i = 1 to N:
- **Update velocity:**
  $\mathbf{v}_i \leftarrow w \times \mathbf{v}_i + c_1 \times \text{rand}() \times (\mathbf{pbest}_i - \mathbf{x}_i) + c_2 \times \text{rand}() \times (\mathbf{gbest} - \mathbf{x}_i)$
- **Update position:**
  $\mathbf{x}_i \leftarrow \mathbf{x}_i + \mathbf{v}_i$
  Clamp $\mathbf{x}_i$ within bounds $[K_p, K_i, Kd]$
- **Evaluate cost:** J_i = ISE(PID with $\mathbf{x}_i$)
- **If** $J_i < J\_\mathbf{pbest}_i$:
  - $\mathbf{pbest}_i \leftarrow \mathbf{x}_i$
  - $J\_\mathbf{pbest}_i \leftarrow J_i$
- **If** $J\_\mathbf{pbest}_i < J\_\mathbf{gbest}$:
  - $\mathbf{gbest} \leftarrow \mathbf{pbest}_i$
  - $J\_\mathbf{gbest} \leftarrow J\_\mathbf{pbest}_i$

Return final solution:
- **Optimal PID gains**: $\mathbf{gbest} = [K_p, K_i, Kd]$
- **Minimum cost**: $J\_\mathbf{gbest}$

Fig. 8. Pseudocode of particle swarm optimization (PSO) applied for PID gain tuning in servo motor control

3.1. Step Input Response

The efficacy of the MG996R servo motor control system was evaluated through simulation and experiments with a 10-degree step input. Four control systems were evaluated: (1) a factory-default internal proportional control, (2) a PID controller optimized via Particle Swarm Optimization (PSO), (3) a manually calibrated proportional-derivative (PD) controller, and (4) a PSO-optimized PID controller augmented with a feedforward component. Standard criteria were used to evaluate the controllers, encompassing rise time, settling time, percent overrun (%OS), root mean square error (RMSE), and mean absolute error (MAE).

The simulation results in Fig. 10 and Table 1 demonstrate that the PSO-tuned PID controller with feedforward compensation exhibited the most optimal overall performance. This controller achieved the lowest RMSE (1.0058°) and MAE (0.1890°), as well as a swift rise time of 0.02 seconds and no

overshoot. The feedforward term's predictive nature allowed it to preemptively counteract changes in the reference trajectory, thereby reducing the effects of motor inertia and phase latency during transient periods. In simulation, the standalone PSO-optimized PID controller (no feedforward) also exhibited satisfactory performance, with an RMSE of 1.0648° and an MAE of 0.2935°. Nevertheless, it required a protracted settling time of 0.50 seconds. The factory-default controller demonstrated the least robust performance, with an MAE of 2.2177° and a 9.02% overshoot. The manually tuned PD controller mitigated overshoot in the interim; however, it continued to experience steady-state error, with an MAE of 1.6460°, which is likely the consequence of insufficient integral compensation.

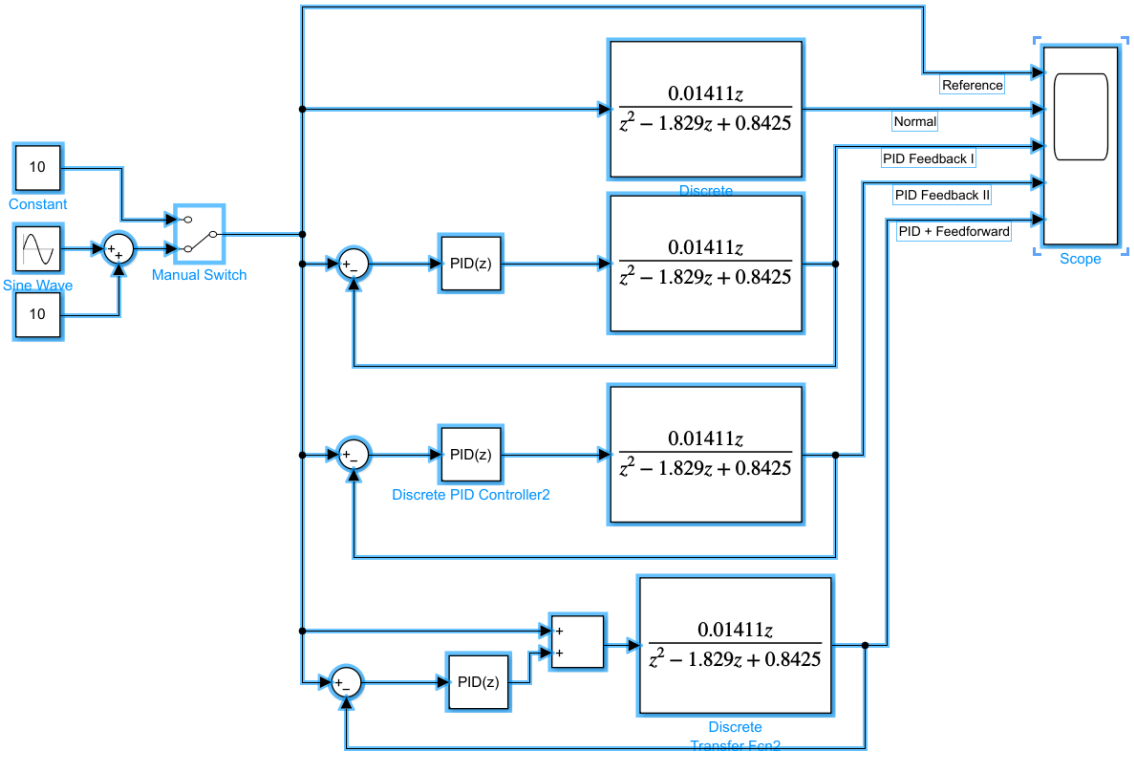

Fig. 9. Simulink block diagram for servo motor testing using different control schemes under step and sine wave inputs

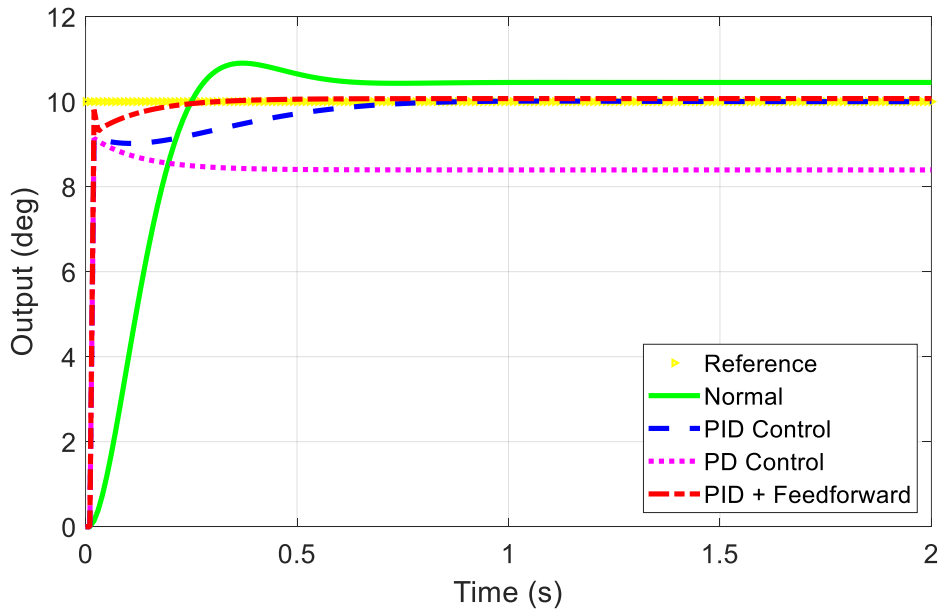

Fig. 10. Simulation responses under 10-degree step input

Table 1. Simulation performance comparison of controllers

Controller	Risetime (Sec)	Setting time (Sec)	%OS (%)	RMSE (deg)	MAE (deg)
Factory Default (Internal P Control)	0.25	0.60	9.02	2.2177	2.2177
PSO-Tuned PID Controller	0.02	0.50	0.00	1.0648	0.2935
Manually Tuned PD Controller	0.02	0.50	0.00	1.8509	1.6460
PSO-Tuned PID + Feedforward Controller	0.02	0.12	0.00	1.0058	0.1890

Table 2 and Fig. 11 illustrate the outcomes of hardware implementation. The PSO-tuned PID controller with feedforward once again surpassed other methods, obtaining the lowest experimental MAE of 0.8497° and a rapid rise time of 0.09 seconds. Nevertheless, it demonstrated a 60% excess that was visible, suggesting that while the system responded quickly, damping was insufficient to eliminate overshoot under real-world disturbances. In contrast, the PSO-tuned PID controller without feedforward was unstable in real-world conditions, exhibiting a substantially high overshoot of 300% and an MAE of 11.5699°. This instability underscores the excessive influence of integral gain (K_i) on physical systems, particularly those that are impacted by mechanical noise and nonlinearities. The PD controller that was manually calibrated demonstrated moderate performance (MAE = 5.1273°), whereas the factory-default controller remained stable but imprecise (MAE = 2.1336°).

Although the system identification process assumes linear behavior, real-world servo motors like the MG996R are known to exhibit nonlinearities due to gear backlash, dead-zone effects in PWM interpretation, and sensor noise. These unmodeled dynamics may contribute to deviations between simulated and experimental responses. Future work may include quantitative modeling of these effects.

In summary, the PSO-optimized PID controller with feedforward achieved optimal performance in both simulation and real-world testing. However, some excess was observed as a result of unmodeled real-world dynamics. Nevertheless, it continues to be the most effective approach for applications that necessitate sub-degree precision, including low-cost medical robot systems, prosthetic actuators, and robotic joints.

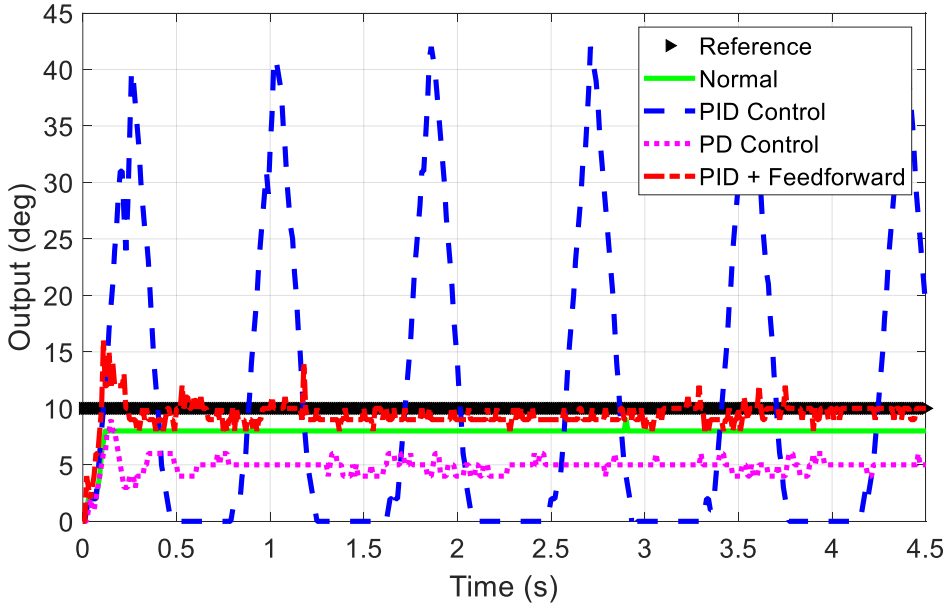

Fig. 11. Experimental responses under 10-degree step input

3.2. Sine Wave Input Response

The effectiveness of all controller topologies in tracking dynamic reference signals was assessed via modeling and experimental testing using a sine wave input with an angular frequency of 2 rad/s

(about 0.318 Hz). Fig. 12 illustrates that the PSO-optimized PID controller with feedforward attained enhanced stability and precision relative to all other methods. It precisely followed the designated sinusoidal trajectory without phase lag or amplitude distortion, achieving the minimal simulated RMSE of 0.5313° and MAE of 0.1630°.

Table 2. Experimental performance comparison of controllers

Controller	Risetime (Sec)	Setting time (Sec)	%OS (%)	RMSE (deg)	MAE (deg)
Factory Default (Internal P Control)	0.12	0.12	0.00	2.3190	2.1336
PSO-Tuned PID Controller	0.10	-	300	13.4692	11.5699
Manually Tuned PD Controller	0.13	0.35	0.00	5.2008	5.1273
PSO-Tuned PID + Feedforward Controller	0.09	0.18	60	1.4340	0.8497

The independent PSO-tuned PID controller demonstrated notable performance (RMSE = 0.7574°, MAE = 0.5211°), albeit its precision was slightly inferior to that of the feedforward-enhanced version. Conversely, the manually calibrated PD controller displayed the poorest simulation performance (RMSE = 2.1548°, MAE = 1.8132°), whereas the factory-default internal P controller showed acceptable accuracy (RMSE = 2.0829°, MAE = 1.6326°), as outlined in Table 3. The performance limitations of the PD controller mostly stem from its lack of integral action and insufficient compensation for phase lag at high frequencies.

The improved effectiveness of the feedforward-augmented controller stems from its ability to proactively counteract expected reference variations, hence enhancing system responsiveness and markedly reducing phase delay in dynamic signal tracking.

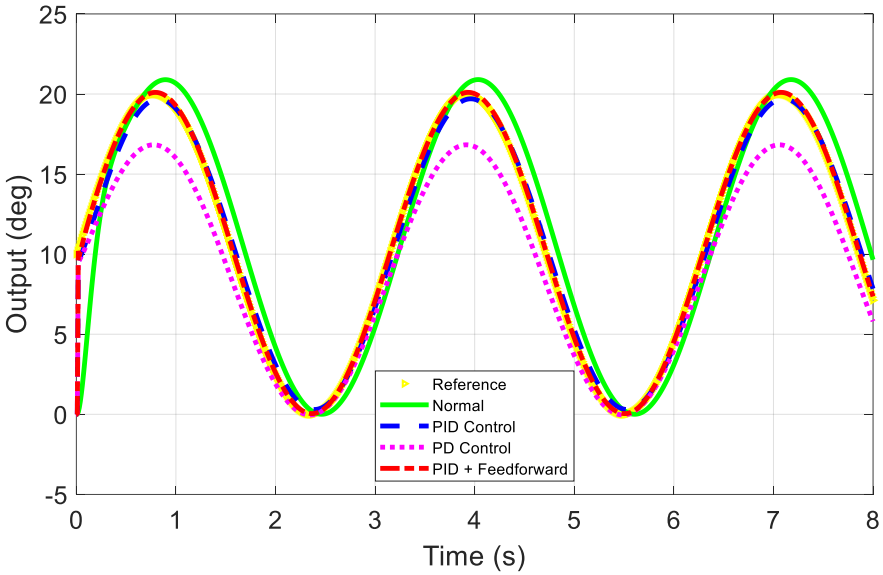

Fig. 12. Simulated Response of Controllers under 2 rad/s Sine Input

Table 3. Simulation Performance Comparison under 2 rad/s Sine Input

Controller	RMSE (deg)	MAE (deg)
Factory Default (Internal P Control)	2.0829	1.6326
PSO-Tuned PID Controller	0.7574	0.5211
Manually Tuned PD Controller	2.1548	1.8132
PSO-Tuned PID + Feedforward Controller	0.5313	0.1630

These trends were largely corroborated by the experimental outcomes, as shown in Fig. 13. However, the physical MG996R system's unmodeled dynamics, sensor noise, and actuator

nonlinearities resulted in significantly higher tracking errors across all controllers. The PSO-PID + feedforward controller maintained its superior performance in real-world conditions, with an RMSE of 4.8711° and an MAE of 3.4042°, surpassing the other controllers by a substantial margin. The PD controller that was manually tuned achieved a second-place ranking (RMSE = 10.9606°, MAE = 9.9792°), surpassing the factory-default control (RMSE = 8.1482°, MAE = 7.1284°).

In contrast, the PSO-PID controller without feedforward experienced significant instability during sine tracking, resulting in RMSE = 25.7527° and MAE = 22.0700°. The large fluctuations were attributed to an excessive integral gain. The critical function of feedforward compensation in suppressing integral windup and enhancing dynamic response, particularly under high-frequency oscillations, is reaffirmed by these findings.

The control design did not account for mechanical backlash, PWM dead-zone effects, and analog sensor noise in the MG996R, which is the primary reason for the performance gap between simulation and real-world evaluations. In order to improve the robustness of real-time controllers, it may be necessary to characterize these nonlinearities in future research.

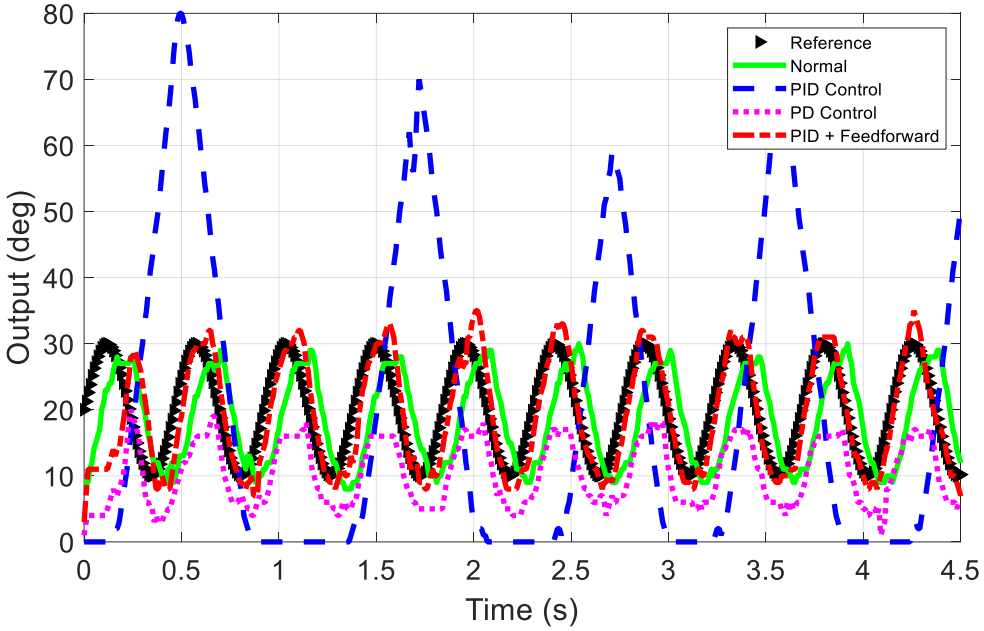

Fig. 13. Experimental Response of Controllers under 2 rad/s Sine Input

In conclusion, the PSO-optimized PID controller with feedforward consistently outperformed all other methods in both simulation and experimental environments, particularly under dynamic sinusoidal conditions. Although the simulation data indicated that the tracking was nearly ideal, the real-world results underscored the necessity of implementing predictive feedforward elements to reduce phase lag and mechanical imperfections. This renders the proposed control strategy highly appropriate for embedded motion control systems that necessitate sub-degree precision, including low-cost biomedical robotics, surgical manipulators, and prosthetic limbs.

3.3. Experimental Comparison and Observations

The gain parameters that were initially determined through Particle Swarm Optimization (PSO) simulations required a four-fold downscaling during validation on the actual MG996R servo motor hardware. The system's dynamic behavior and stability were substantially impacted by practical constraints, such as intrinsic nonlinearities, internal friction, actuator saturation, and sensor noise. Consequently, this adjustment was necessary.

The controller performance evaluations remained consistent between simulations and physical experiments, despite the fact that gain scaling was implemented (see Table 2 and Table 4, Fig. 11

and Fig. 13). In both steady-state and oscillatory tracking conditions, the PSO-optimized PID controller with feedforward consistently outperformed other methods. Conversely, the standalone PSO-tuned PID controller, which demonstrated exceptional performance in simulation, demonstrated significant instability during hardware implementation. The embedded system's real-time processing capabilities and precision limits were surpassed by the excessively high integral gain (K_i), which is the primary cause of this issue.

Table 4. Experimental performance comparison under 2 rad/s sine input

Controller	RMSE (deg)	MAE (deg)
Factory Default (Internal P Control)	8.1482	7.1284
PSO-Tuned PID Controller	25.7527	22.0700
Manually Tuned PD Controller	10.9606	9.9792
PSO-Tuned PID + Feedforward Controller	4.8711	3.4042

This observation emphasizes the importance of meticulously validating and scaling controller gains derived from simulations prior to real-world deployment, particularly in systems with fixed internal logic and constrained bandwidth. The factory-default proportional controller exhibited excellent stability but lacked precision, whereas the manually tuned PD controller exhibited moderate performance. Although these methods are functional, they are not robust in diverse operating conditions and necessitate extensive manual calibration.

Tracking accuracy with a mean absolute error (MAE) below 1° is generally considered acceptable to assure smooth, safe actuator behavior, as per the typical requirements of biomedical robotics and prosthetics. In this investigation, the PSO-PID with feedforward controller obtained an MAE of 0.8497° under step input conditions, thereby validating its suitability for sub-degree precision challenges.

Nevertheless, this method resulted in a 60% overshoot during experimental tests, despite the fact that it provided a rapid response and precise monitoring. This trade-off underscores a prevalent control design compromise: the prioritization of rise time and responsiveness may be at the expense of attenuation. In order to mitigate overshoot and guarantee mechanical protection, it may be necessary to implement additional suspension, safety margins, or adaptive gain scheduling in safety-critical applications, such as surgical robotics or prosthetic limbs.

In general, the integration of feedforward elements into PSO-based PID architectures is a practicable and effective approach to enhancing control precision in constrained servo motor systems, such as the MG996R.

4. Conclusion

The control accuracy of factory-locked MG996R servo motors was enhanced in this study by employing a PSO-optimized PID controller with feedforward compensation, which was non-invasive. The proposed technique, in contrast to conventional methods that require internal modification, externally accessed the built-in potentiometer, which was originally intended for internal position feedback, without any modification to the servo's internal circuitry. This enabled the real-time acquisition of angular position data, thereby preserving hardware integrity and enabling precise external control. The feedforward-enhanced configuration consistently exhibited superior performance in both simulation and hardware validation out of the four control strategies that were evaluated in comparison to the factory-default P control, manually tuned PD control, standalone PSO-tuned PID, and PSO-PID with feedforward. The RMSE and MAE of both sinusoidal and step stimuli were substantially diminished. Nevertheless, the standalone PSO-PID controller was problematic in real-world conditions as a result of excessive integral action, despite its effectiveness in simulation. This underscores the significance of scalability gain in the deployment of embedded platforms.

Tracking errors of 1–2° are frequently tolerable in biomedical systems, such as assistive robotic appendages, surgical manipulators, and prosthetic joints. This technique is particularly relevant in these applications. Although certain test cases demonstrated a mean absolute error of less than 1°, practical constraints, including actuator nonlinearities and overshoot, indicate that further refinement is necessary. This approach has the potential to be further developed to facilitate robust, real-time control in safety-critical embedded applications by incorporating compensation for gear backlash and PWM dead zones and developing adaptive gain tuning. Additionally, future research may focus on the extension of this methodology to multi-axis control systems.

Author Contribution: All authors contributed equally to the main contributor to this paper. All authors read and approved the final paper.

Funding: Research Institute, Academic Services Center, and College of Biomedical Engineering, Rangsit University.

Acknowledgment: The researcher would like to thank the Research Institute, Academic Services Center, and College of Biomedical Engineering, Rangsit University for the grant of research funding to the research team. Furthermore, it is confirmed that the project has been reviewed by the Ethics Review Board of Rangsit University, with reference number RSUERB2025-006, which certifies that the research does not involve human subjects. Moreover, AI-driven methods (QuillBot Premium) were utilized for grammatical verification, paraphrasing, and linguistic augmentation to ensure the accuracy and clarity of the text.

Conflicts of Interest: The authors declare no conflict of interest.

References

[1] A. Latif, A. Z. Arfianto, H. A. Widodo, R. Rahim, and E. T. Helmy, "Motor DC PID System Regulator for Mini Conveyor Drive Based on MATLAB," *Journal of Robotics and Control (JRC)*, vol. 1, no. 6, pp. 185-190, 2020, https://doi.org/10.18196/jrc.1636.

[2] S. Mahfoud, A. Derouich, N. El Ouanjli, M. El Mahfoud, and M. Taoussi, "A New Strategy-Based PID Controller Optimized by Genetic Algorithm for DTC of the Doubly Fed Induction Motor," *Systems*, vol. 9, no. 2, p. 37, 2021, https://doi.org/10.3390/systems9020037.

[3] P. Chotikunnan and R. Chotikunnan, "Dual design PID controller for robotic manipulator application," *Journal of Robotics and Control (JRC)*, vol. 4, no. 1, pp. 23-34, 2023, https://doi.org/10.18196/jrc.v4i1.16990.

[4] F. N. Abdullah, G. A. Aziz, and S. W. Shneen, "GWO-PID of two-phase hybrid stepping motor for robotic grinding force," *Journal of Fuzzy Systems and Control*, vol. 1, no. 3, pp. 71–79, 2023, https://doi.org/10.59247/jfsc.v1i3.91.

[5] K. Rahimunnisa, M. Atchaiya, B. Arunachalam, and V. Divyaa, "AI-based smart and intelligent wheelchair," *Journal of Applied Research and Technology*, vol. 18, no. 6, pp. 362-367, 2020, https://doi.org/10.22201/icat.24486736e.2020.18.6.1351.

[6] E. S. Ghith and F. A. A. Tolba, "Design and optimization of PID controller using various algorithms for micro-robotics system," *Journal of Robotics and Control (JRC)*, vol. 3, no. 3, pp. 244-256, 2022, https://doi.org/10.18196/jrc.v3i3.14827.

[7] S. J. Hammoodi, K. S. Flayyih, and A. R. Hamad, "Design and Implementation of Speed Control System for DC Motor Based on PID Control and Matlab Simulink," *International Journal of Power Electronics and Drive Systems*, vol. 11, no. 1, pp. 127-134, 2020, http://doi.org/10.11591/ijpeds.v11.i1.pp127-134.

[8] D. S. Febriyan and R. D. Puriyanto, "Implementation of DC motor PID control on conveyor for separating potato seeds by weight," *International Journal of Robotics and Control Systems*, vol. 1, no. 1, pp. 15-26, 2021, https://doi.org/10.31763/ijrcs.v1i1.221.

[9] C. Wulandari and A. Fadlil, "Center of pressure control for balancing humanoid dance robot using load cell sensor, Kalman filter and PID controller," *Control Systems and Optimization Letters*, vol. 1, no. 2, pp. 75-81, 2023, https://doi.org/10.59247/csol.v1i2.22.

[10] E. W. Suseno and A. Ma'arif, "Tuning of PID controller parameters with genetic algorithm method on DC motor," *International Journal of Robotics and Control Systems*, vol. 1, no. 1, pp. 41-53, 2021, https://doi.org/10.31763/ijrcs.v1i1.249.

[11] R. P. Borase, D. K. Maghade, S. Y. Sondkar, and S. N. Pawar, "A review of PID control, tuning methods and applications," *International Journal of Dynamics and Control*, vol. 9, no. 2, pp. 818-827, 2021, https://doi.org/10.1007/s40435-020-00665-4.

[12] R. R. Alla, N. Lekyasri, and K. Rajani, "PID Control Design for Second Order Systems," *International Journal of Engineering and Manufacturing*, vol. 9, no. 4, pp. 45-56, 2019, https://doi.org/10.5815/ijem.2019.04.04.

[13] E. S. Rahayu, A. Ma'arif, and A. Çakan, "Particle swarm optimization (PSO) tuning of PID control on DC motor," *International Journal of Robotics and Control Systems*, vol. 2, no. 2, pp. 435-447, 2022, https://doi.org/10.31763/ijrcs.v2i2.476.

[14] Z. Qi, Q. Shi and H. Zhang, "Tuning of Digital PID Controllers Using Particle Swarm Optimization Algorithm for a CAN-Based DC Motor Subject to Stochastic Delays," *IEEE Transactions on Industrial Electronics*, vol. 67, no. 7, pp. 5637-5646, 2020, https://doi.org/10.1109/TIE.2019.2934030.

[15] C. T. Chao, N. Sutarna, J. S. Chiou, and C. J. Wang, "An optimal fuzzy PID controller design based on conventional PID control and nonlinear factors," *Applied Sciences*, vol. 9, no. 6, p. 1224, 2019, https://doi.org/10.3390/app9061224.

[16] H. Maghfiroh, A. Ramelan, and F. Adriyanto, "Fuzzy-PID in BLDC motor speed control using MATLAB/Simulink," *Journal of Robotics and Control (JRC)*, vol. 3, no. 1, pp. 8-13, 2022, https://doi.org/10.18196/jrc.v3i1.10964.

[17] N. Ramadhani, A. Ma'arif, and A. Çakan, "Implementation of PID control for angular position control of Dynamixel servo motor," *Control Systems and Optimization Letters*, vol. 2, no. 1, pp. 8–14, 2024, https://doi.org/10.59247/csol.v2i1.40.

[18] O. T. Altinoz and A. E. Yilmaz, "Investigation of the Optimal PID-Like Fuzzy Logic Controller for Ball and Beam System with Improved Quantum Particle Swarm Optimization," *International Journal of Computational Intelligence and Applications*, vol. 21, no. 04, p. 2250025, 2022, https://doi.org/10.1142/S1469026822500250.

[19] M. Jain, V. Saihjpal, N. Singh, and S. B. Singh, "An overview of variants and advancements of PSO algorithm," *Applied Sciences*, vol. 12, no. 17, p. 8392, 2022, https://doi.org/10.3390/app12178392.

[20] B. Song, R. Wang, and L. Xu, "Design of PMSM Dual-Loop Control Systems Integrating LADRC and PI Controllers via an Improved PSO Algorithm," *International Transactions on Electrical Energy Systems*, 2024, https://doi.org/10.1155/2024/9378284.

[21] D. S. Febriyan and R. D. Puriyanto, "Implementation of DC motor PID control on conveyor for separating potato seeds by weight," *International Journal of Robotics and Control Systems*, vol. 1, no. 1, pp. 15–26, 2021, https://doi.org/10.31763/ijrcs.v1i1.221.

[22] M. M. Nishat, F. Faisal, A. J. Evan, M. M. Rahaman, M. S. Sifat, and H. F. Rabbi, "Development of Genetic Algorithm (GA) Based Optimized PID Controller for Stability Analysis of DC-DC Buck Converter," *Journal of Power and Energy Engineering*, vol. 8, no. 09, pp. 8-19, 2020, https://doi.org/10.4236/jpee.2020.89002.

[23] K. Vanchinathan and N. Selvaganesan, "Adaptive Fractional Order PID Controller Tuning for Brushless DC Motor Using Artificial Bee Colony Algorithm," *Results in Control and Optimization*, vol. 4, p. 100032, 2021, https://doi.org/10.1016/j.rico.2021.100032.

[24] D. D. Ramírez-Ochoa, L. A. Pérez-Domínguez, E. A. Martínez-Gómez, and D. Luviano-Cruz, "PSO, a swarm intelligence-based evolutionary algorithm as a decision-making strategy: A review," *Symmetry*, vol. 14, no. 3, p. 455, 2022, https://doi.org/10.3390/sym14030455.

[25] M. G. Abdolrasol, A. Ayob, A. H. Mutlag, and T. S. Ustun, "Optimal fuzzy logic controller based PSO for photovoltaic system," *Energy Reports*, vol. 9, pp. 427–434, 2023, https://doi.org/10.1016/j.egyr.2022.11.039.

[26] V. Velmurugan, M. Venkatesan, and N. Praboo, "Analysis and performance validation of CRONE controllers for speed control of a DC motor," *International Journal of Robotics and Control Systems*, vol. 4, no. 2, pp. 558–580, 2024, https://doi.org/10.31763/ijrcs.v4i2.1343.

[27] P. Mohindru, "Review on PID, fuzzy and hybrid fuzzy PID controllers for controlling non-linear dynamic behaviour of chemical plants," *Artificial Intelligence Review*, vol. 57, p. 97, 2024, https://doi.org/10.1007/s10462-024-10743-0.

[28] S. Gobinath and M. Madheswaran, "Deep Perceptron Neural Network with Fuzzy PID Controller for Speed Control and Stability Analysis of BLDC Motor," *Soft Computing*, vol. 24, no. 13, pp. 10161-10180, 2020, https://doi.org/10.1007/s00500-019-04532-z.

[29] P. Chotikunnan, R. Chotikunnan, A. Nirapai, A. Wongkamhang, P. Imura, and M. Sangworasil, "Optimizing Membership Function Tuning for Fuzzy Control of Robotic Manipulators Using PID-Driven Data Techniques," *Journal of Robotics and Control (JRC)*, vol. 4, no. 2, pp. 128-140, 2023, https://doi.org/10.18196/jrc.v4i2.18108.

[30] J. S. Wang and C. G. Lee, "Self-adaptive neuro-fuzzy inference systems for classification applications," *IEEE Transactions on Fuzzy systems*, vol. 10, no. 6, pp. 790-802, 2002, https://doi.org/10.1109/TFUZZ.2002.805880.

[31] M. Kiew-ong-art, P. Chotikunnan, A. Wongkamhang, R. Chotikunnan, A. Nirapai, P. Imura, M. Sangworasil, N. Thongpance, and A. Srisiriwat, "Comparative Study of Takagi-Sugeno-Kang and Madani Algorithms in Type-1 and Interval Type-2 Fuzzy Control for Self-Balancing Wheelchairs," *International Journal of Robotics and Control Systems*, vol. 3, no. 4, pp. 643-657, 2023, https://doi.org/10.31763/ijrcs.v3i4.1154.

[32] F. Umam, A. Dafid, and A. D. Cahyani, "Implementation of Fuzzy Logic Control Method on Chilli Cultivation Technology Based Smart Drip Irrigation System," *Jurnal Ilmiah Teknik Elektro Komputer dan Informatika*, vol. 9, no. 1, pp. 132-141, 2023, https://doi.org/10.26555/jiteki.v9i1.25878.

[33] A. M. Lopes and L. Chen, "Fractional order systems and their applications," *Fractal and Fractional*, vol. 6, no. 7, p. 389, 2022, https://doi.org/10.3390/fractalfract6070389.

[34] D. Li and J. Dong, "Fractional-Order Systems Optimal Control via Actor-Critic Reinforcement Learning and Its Validation for Chaotic MFET," *IEEE Transactions on Automation Science and Engineering*, vol. 22, pp. 1173-1182, 2025, https://doi.org/10.1109/TASE.2024.3361213.

[35] K. Sayed, H. H. El-Zohri, A. Ahmed, and M. Khamies, "Application of Tilt Integral Derivative for Efficient Speed Control and Operation of BLDC Motor Drive for Electric Vehicles," *Fractal and Fractional*, vol. 8, no. 1, p. 61, 2024, https://doi.org/10.3390/fractalfract8010061.

[36] V. Kumarasamy, V. KarumanchettyThottam Ramasamy, G. Chandrasekaran, *et al*., "A review of integer order PID and fractional order PID controllers using optimization techniques for speed control of brushless DC motor drive," *International Journal of System Assurance Engineering and Management*, vol. 14, pp. 1139–1150, 2023, https://doi.org/10.1007/s13198-023-01952-x.

[37] Z. U. A. Zafar, N. Ali, and C. Tunç, "Mathematical modeling and analysis of fractional-order brushless DC motor," *Advances in Difference Equations*, vol. 2021, no. 433, 2021, https://doi.org/10.1186/s13662-021-03587-3.

[38] T.-B. Tran *et al*., "Trajectory tracking using LQR control for Pendubot: Simulation and experiment," *Journal of Fuzzy Systems and Control*, vol. 2, no. 1, pp. 18–21, 2024, https://doi.org/10.59247/jfsc.v2i1.163.

[39] P. Dutta and S. K. Nayak, "Grey Wolf Optimizer Based PID Controller for Speed Control of BLDC Motor," *Journal of Electrical Engineering & Technology*, vol. 16, no. 2, pp. 955-961, 2021, https://doi.org/10.1007/s42835-021-00660-5.

[40] S. Wang, X. Zhao, and Q. Yu, "Vehicle stability control strategy based on recognition of driver turning intention for dual-motor drive electric vehicle," *Mathematical Problems in Engineering*, 2020, https://doi.org/10.1155/2020/3143620.

[41] V. Shukla, B. Singh and S. Patil, "The Development of Bio-Inspired Snake Robot," *2023 IEEE Engineering Informatics*, pp. 1-7, 2023, https://doi.org/10.1109/IEEECONF58110.2023.10520602.

[42] C. -T. Hsieh, "Joystick-based Motion Control for 6-Axis Low Cost Robot Arm," *2023 International Conference on Fuzzy Theory and Its Applications (iFUZZY)*, pp. 1-4, 2023, https://doi.org/10.1109/iFUZZY60076.2023.10324130.

[43] A. Ma'arif and N. R. Setiawan, "Control of DC motor using integral state feedback and comparison with PID: simulation and Arduino implementation," *Journal of Robotics and Control (JRC)*, vol. 2, no. 5, pp. 456-461, 2021, https://doi.org/10.18196/jrc.25122.

[44] T. Y. Wu, Y. Z. Jiang, Y. Z. Su, and W. C. Yeh, "Using Simplified Swarm Optimization on Multiloop Fuzzy PID Controller Tuning Design for Flow and Temperature Control System," *Applied Sciences*, vol. 10, no. 23, p. 8472, 2020, https://doi.org/10.3390/app10238472.

[45] H. Torres-Salinas, J. Rodríguez-Reséndiz, E. E. Cruz-Miguel, and L. A. Ángeles-Hurtado, "Fuzzy logic and genetic-based algorithm for a servo control system," *Micromachines*, vol. 13, no. 4, p. 586, 2022, https://doi.org/10.3390/mi13040586.

[46] M. Luo, J. A. Duan, and Z. Yi, "Speed tracking performance for a coreless linear motor servo system based on a fitted adaptive fuzzy controller," *Energies*, vol. 16, no. 3, p. 1259, 2023, https://doi.org/10.3390/en16031259.

[47] E. H. Kadhim and A. T. Abdulsadda, "Mini drone linear and nonlinear controller system design and analyzing," *Journal of Robotics and Control (JRC)*, vol. 3, no. 2, pp. 212-218, 2022, https://doi.org/10.18196/jrc.v3i2.14180.

[48] A. K. Hado, B. S. Bashar, M. M. A. Zahra, R. Alayi, Y. Ebazadeh, and I. Suwarno, "Investigating and optimizing the operation of microgrids with intelligent algorithms," *Journal of Robotics and Control (JRC)*, vol. 3, no. 3, pp. 279-288, 2022, https://doi.org/10.18196/jrc.v3i3.14772.

[49] D. Kumar, R. Malhotra, and S. R. Sharma, "Design and construction of a smart wheelchair," *Procedia Computer Science*, vol. 172, pp. 302-307, 2020, https://doi.org/10.1016/j.procs.2020.05.048.

[50] M. R. Islam, M. R. T. Hossain, and S. C. Banik, "Synchronizing of stabilizing platform mounted on a two-wheeled robot," *Journal of Robotics and Control (JRC)*, vol. 2, no. 6, pp. 552-558, 2021, https://doi.org/10.18196/26136.

[51] A. O. Amole, O. E. Olabode, D. O. Akinyele, and S. G. Akinjobi, "Optimal Temperature Control Scheme for Milk Pasteurization Process Using Different Tuning Techniques for a Proportional Integral Derivative Controller," *Iranian Journal of Electrical and Electronic Engineering*, vol. 18, no. 3, pp. 1-16, 2022, https://ijeee.iust.ac.ir/article-1-2170-en.pdf.

[52] P. Saini and C. Sharma, "Comparative Analysis of Controller Tuning Techniques for Dead Time Processes," *International Journal of Mathematical, Engineering and Management Sciences*, vol. 4, no. 3, p. 803, 2019, https://doi.org/10.33889/IJMEMS.2019.4.3-063.

[53] S. W. Shneen, H. S. Dakheel, and Z. B. Abdullah, "Design and implementation of no load, constant and variable load for DC servo motor," *Journal of Robotics and Control (JRC)*, vol. 4, no. 3, pp. 323–329, 2023, https://doi.org/10.18196/jrc.v4i3.17387.

[54] M. A. Abdelghany, A. O. Elnady, and S. O. Ibrahim, "Optimum PID controller with fuzzy self-tuning for DC servo motor," *Journal of Robotics and Control (JRC)*, vol. 4, no. 4, pp. 500–508, 2023, https://doi.org/10.18196/jrc.v4i4.18676.

[55] A. Sharkawy and J. Nazzal, "Design and manufacturing using 3D printing technology of a 5-DOF manipulator for industrial tasks," *International Journal of Robotics and Control Systems*, vol. 4, no. 2, pp. 893–909, 2024, https://doi.org/10.31763/ijrcs.v4i2.1456.

[56] A. W. Hidayat, I. Sulistiyowati, A. Wicaksono, and S. Syahrorini, "Hybrid system prototype for dam water level control system to irrigating rice fields," *Buletin Ilmiah Sarjana Teknik Elektro*, vol. 6, no. 1, pp. 25–33, 2024, https://doi.org/10.12928/biste.v6i1.10016.

[57] K. Kunal, A. Z. Arfianto, J. E. Poetro, F. Waseel, and R. A. Atmoko, "Accelerometer implementation as feedback on 5 degree of freedom arm robot," *Journal of Robotics and Control (JRC)*, vol. 1, no. 1, pp. 31–34, 2020, https://doi.org/10.18196/jrc.1107.

[58] F. Ahmmed, A. Rahman, A. Islam, A. Alaly, S. Mehnaj, P. Saha, and T. Hossain, "Arduino-controlled multi-function robot with Bluetooth and nRF24L01+ communication," *International Journal of Robotics and Control Systems*, vol. 4, no. 3, pp. 1353–1381, 2024, https://doi.org/10.31763/ijrcs.v4i3.1517.

[59] A. Prasetyo, J. Jamaaluddin, and I. Anshory, "PCB (Printed Circuit Board) etching machine using ESP32-Camera based Internet of Things," *Buletin Ilmiah Sarjana Teknik Elektro*, vol. 5, no. 2, pp. 260–268, 2023, https://doi.org/10.12928/biste.v5i2.8132.

[60] Y. Irawan, M. Muhardi, R. Ordila, and R. Diandra, "Automatic floor cleaning robot using Arduino and ultrasonic sensor," *Journal of Robotics and Control (JRC)*, vol. 2, no. 4, pp. 240–243, 2021, https://doi.org/10.18196/jrc.2485.

[61] Y. Irawan, R. Wahyuni, and H. Fonda, "Folding clothes tool using Arduino Uno microcontroller and gear servo," *Journal of Robotics and Control (JRC)*, vol. 2, no. 3, pp. 170–174, 2021, https://doi.org/10.18196/jrc.2373.

[62] M. H. Zulwidad and I. Sulistiyowati, "Efficiency through automation: A single system for multiple railway guard posts," *Buletin Ilmiah Sarjana Teknik Elektro*, vol. 5, no. 3, pp. 407–416, 2023, https://doi.org/10.12928/biste.v5i3.9001.

[63] T. Triwiyanto, W. Caesarendra, V. Abdullayev, A. A. Ahmed, and H. Herianto, "Single lead EMG signal to control an upper limb exoskeleton using embedded machine learning on Raspberry Pi," *Journal of Robotics and Control (JRC)*, vol. 4, no. 1, pp. 35–45, 2023, https://doi.org/10.18196/jrc.v4i1.17364.

[64] A. Juliano, A. H. Hendrawan, and R. Ritzkal, "Information system prototyping of strawberry maturity stages using Arduino Uno and TCS3200," *Journal of Robotics and Control (JRC)*, vol. 1, no. 3, pp. 86–91, 2020, https://doi.org/10.18196/jrc.1319.

[65] A. Muqaffi Siswanto and M. Muchlas, "Prototype of automatic sorting of goods in cosmetics warehouse," *Buletin Ilmiah Sarjana Teknik Elektro*, vol. 4, no. 3, pp. 142–151, 2023, https://doi.org/10.12928/biste.v4i3.6919.

[66] K. Khairunisa, M. Mardeni, and Y. Irawan, "Smart aquarium design using Raspberry Pi and Android based," *Journal of Robotics and Control (JRC)*, vol. 2, no. 5, pp. 368–372, 2021, https://doi.org/10.18196/jrc.25109.

[67] A. A. Sahrab and H. M. Marhoon, "Design and fabrication of a low-cost system for smart home applications," *Journal of Robotics and Control (JRC)*, vol. 3, no. 4, pp. 409–414, 2022, https://doi.org/10.18196/jrc.v3i4.15413.

[68] F. N. Abdullah, G. A. Aziz, and S. W. Shneen, "Simulation model of servo motor by using MATLAB," *Journal of Robotics and Control (JRC)*, vol. 3, no. 2, pp. 176–179, 2022, https://doi.org/10.18196/jrc.v3i2.13959.